

# Evidence for ferritin as dominant iron-bearing species in the rhizobacterium *Azospirillum brasilense* Sp7 provided by low-temperature/in-field Mössbauer spectroscopy

Krisztina Kovács<sup>1</sup> · Alexander A. Kamnev<sup>2</sup> · Jiří Pechoušek<sup>3</sup> · Anna V. Tugarova<sup>2</sup> · Ernő Kuzmann<sup>1</sup> · Libor Machala<sup>3</sup> · Radek Zbořil<sup>3</sup> · Zoltán Homonnay<sup>1</sup> · Károly Lázár<sup>4</sup>

Received: 7 August 2015 / Revised: 3 December 2015 / Accepted: 9 December 2015 / Published online: 14 January 2016  
© Springer-Verlag Berlin Heidelberg 2016

**Abstract** For the ubiquitous diazotrophic rhizobacterium *Azospirillum brasilense*, which has been attracting the attention of researchers worldwide for the last 35 years owing to its significant agrobiotechnological and phytostimulating potential, the data on iron acquisition and its chemical speciation in cells are scarce. In this work, for the first time for azospirilla, low-temperature (at 80 K, 5 K, as well as at 2 K without and with an external magnetic field of 5 T) transmission Mössbauer spectroscopic studies were performed for lyophilised biomass of *A. brasilense* (wild-type strain Sp7 grown with <sup>57</sup>Fe<sup>III</sup> nitrilotriacetate complex as the sole source of iron) to enable quantitative chemical speciation analysis of the intracellular iron. In the Mössbauer spectrum at 80 K, a broadened quadrupole doublet of high-spin iron(III) was observed with a few percent of a high-spin iron(II) contribution. In the spectrum measured at 5 K, a dominant magnetically split component appeared with the parameters typical of ferritin species from other bacteria, together with a quadrupole doublet of a superparamagnetic iron(III) component and a similarly small contribution from the high-spin iron(II) com-

ponent. The Mössbauer spectra recorded at 2 K (with or without a 5 T external field) confirmed the assignment of ferritin species. About 20 % of total Fe in the dry cells of *A. brasilense* strain Sp7 were present in iron(III) forms superparamagnetic at both 5 and 2 K, i.e. either different from ferritin cores or as ferritin components with very small particle sizes.

**Keywords** Iron metabolism · Bacterial ferritin · *Azospirillum brasilense* · <sup>57</sup>Fe transmission Mössbauer spectroscopy

## Introduction

Ubiquitous diazotrophic free-living rhizobacteria of the genus *Azospirillum*, and the species *A. brasilense* in particular, can form rhizospheric associative symbioses with various higher plants, promoting their growth and development via different mechanisms including (but not limited to) phytohormone production and atmospheric nitrogen fixation [1–3]. Thus, owing to their significant agrobiotechnological and phytostimulating potential, azospirilla have been attracting the attention of researchers worldwide for the last 35 years [2–4]. This continued interest, particularly to *A. brasilense*, is also due to the fact that this species has both epiphytic strains (e.g. wild-type strain *A. brasilense* Sp7, colonising exclusively the plant root surface) and facultatively endophytic strains (e.g. wild-type strain *A. brasilense* Sp245, capable of penetrating into the plant root tissues) [5]. Thus, such strains of the same species occupy different ecological niches in the rhizospheric soil and therefore have different adaptive behaviour, being a convenient model for studying microbial ecology. As a consequence, strains Sp7 and Sp245 have often been compared and documented to exhibit different responses to the same unfavourable conditions or stress factors [6–11].

✉ Alexander A. Kamnev  
aakamnev@ibppm.sgu.ru; a.a.kamnev@mail.ru

<sup>1</sup> Institute of Chemistry, Eötvös Loránd University, P.O. Box 32, Budapest 1512, Hungary  
<sup>2</sup> Institute of Biochemistry and Physiology of Plants and Microorganisms, Russian Academy of Sciences, Saratov 410049, Russia  
<sup>3</sup> Regional Centre of Advanced Technologies and Materials, Departments of Experimental Physics and Physical Chemistry, Faculty of Science, Palacký University in Olomouc, Olomouc 771 46, Czech Republic  
<sup>4</sup> Centre for Energy Research, Hungarian Academy of Sciences, P.O. Box 49, Budapest 1525, Hungary

Despite the intensive and steadily growing studies related to azospirilla (see, e.g. recent reviews [1–4, 6] and the latest collection of review chapters [12]), there is scarcity of information on iron acquisition, metabolism and chemical speciation in these bacteria [13–16]. It is needless to say that iron plays a paramount and multifaceted role in all organisms, including bacteria (with quite few exceptions). On the basis of the level of iron accumulation in cells of *A. brasilense* (strain Sp245) [16], we recently performed a preliminary study by low-temperature (80 K) transmission Mössbauer spectroscopy which, used for the first time for the bacteria of the genus *Azospirillum*, suggested the presence of a ferritin-like species as one of the components in the iron ‘pool’ in cells of *A. brasilense* strains Sp7 [17] and Sp245 [18] (note that in [17, 18],  $^{57}\text{Fe}$  transmission Mössbauer spectroscopic measurements were performed at 80 K for aqueous suspensions of live bacteria rapidly frozen in liquid nitrogen). This was also complemented by room-temperature high-velocity-resolution Mössbauer measurements on lyophilised biomass of *A. brasilense* strain Sp245 showing heterogeneity of the anticipated iron (hydr)oxide-containing ferritin-like core [19]. Note that in bacteria, three different types of ferritin-like proteins can exist (24-subunit bacterial ferritin, which has a similarity with mammalian ferritin, and heme-containing bacterioferritin, as well as dodecameric DNA-binding ferritin) with variations in the cavity size inside the protein shell and, correspondingly, in the maximum number of iron ions in the core [20, 21].

The aforementioned preliminary data definitely require low-temperature Mössbauer measurements (at  $\leq 5$  K, including in-field measurements as well) to elucidate the correct assignment of the suggested ferritin-like component and other iron-containing species in bacterial cells. This was the primary aim of the present communication, where lyophilised biomass of strain *A. brasilense* Sp7 was used. In order to control the overall composition of the bacterial sample (which was expected to correspond to normal growth conditions without nutritional stress), Fourier transform infrared (FTIR) spectroscopy was used in the diffuse reflectance mode (DRIFT), which is sensitive to fine structural and compositional changes in dried bacterial samples [10, 11, 22].

## Materials and methods

The bacterium (wild-type strain *A. brasilense* Sp7, from The Collection of Rhizosphere Microorganisms, [WDCM 1021], maintained at the Institute of Biochemistry and Physiology of Plants and Microorganisms, RAS, Saratov) was cultivated at 31 °C for 18 h under aeration on a rotary shaker (180 rpm) in a standard phosphate–malate medium as described elsewhere [10, 11, 22], with 0.5 g l<sup>-1</sup> NH<sub>4</sub>Cl as a source of bound nitrogen and 70 μM  $^{57}\text{Fe}^{\text{III}}$  complex with nitrilotriacetic acid

(NTA), equivalent to 4.0 mg l<sup>-1</sup> of isotopically enriched  $^{57}\text{Fe}^{\text{III}}$ , as a sole source of iron for the growing cells. The resulting cells were separated from the culture medium by centrifugation (2370×g, 30 min), washed three times with sterile saline solution (aqueous 0.85 % NaCl), frozen in liquid nitrogen and lyophilised.

To control the overall composition of the bacterial sample, its DRIFT spectrum was obtained and processed using a Nicolet 6700 FTIR spectrometer (Thermo Electron Corporation, USA) with a DRIFT accessory and a Micro sampling cup (Spectra-Tech, USA) as reported elsewhere [10, 11].

Mössbauer measurements at 80 K were carried out with a conventional Mössbauer spectrometer (WISSEL) operating in the constant acceleration mode and equipped with a  $^{57}\text{Co}(\text{Rh})$  source. The sample was kept in a helium cryostat (JANIS SVT-400-MOSS) filled with liquid nitrogen. The experimental data were obtained using a conventional scintillation detector and a computer-operated multichannel analyser (MSPCA Analyser Mössbauer Spectrometer Control and Acquisition Unit). The low-temperature  $^{57}\text{Fe}$  Mössbauer spectra were recorded at 5 and 2 K in zero external magnetic field and at 2 K in a 5 T external magnetic field, using a Spectromag (Oxford Instruments) cryomagnetic system with an MS96 Mössbauer spectrometer [23, 24] attached to the system. The external magnetic field was applied in the parallel geometry with respect to the propagation of the gamma rays. The acquired Mössbauer spectra were recorded with 512 channels and then processed (i.e. by applying noise filtering and fitting). The duration of the measurements was 45, 51 and 44 h for the spectra measured at 5 K, 2 K in zero external magnetic field and 2 K in a 5 T external magnetic field, respectively. For all measurements, the  $^{57}\text{Co}$  source was kept at room temperature.

The Mössbauer spectra were evaluated by the standard computer-based statistical analysis which included fitting the experimental data to a sum of Lorentzians using a least squares minimisation procedure for  $\chi^2$  with the help of the MOSSWINN program [25]. While fitting the magnetic sextets, the line areas were constrained to be 3:1 for the pair of lines (1, 6) relative to lines (3, 4). The linewidths were independent for the pairs of lines (1, 6), (2, 5) and (3, 4).

The values of the isomer shift ( $\delta$ ; mm s<sup>-1</sup> relative to  $\alpha$ -Fe at room temperature), quadrupole splitting ( $\Delta$ , mm s<sup>-1</sup>), linewidth ( $W$ , mm s<sup>-1</sup>; full width at half maximum), internal (or effective) magnetic field ( $B$ , T) and relative areas of spectral components ( $A$ , %) were thus calculated for each spectral component. The linewidth of the  $\alpha$ -Fe calibration foil was 0.30 ± 0.01 mm s<sup>-1</sup>.

## Results and discussion

It is important to note that the bacteria of the genus *Azospirillum* (including *A. brasilense*), being commonly

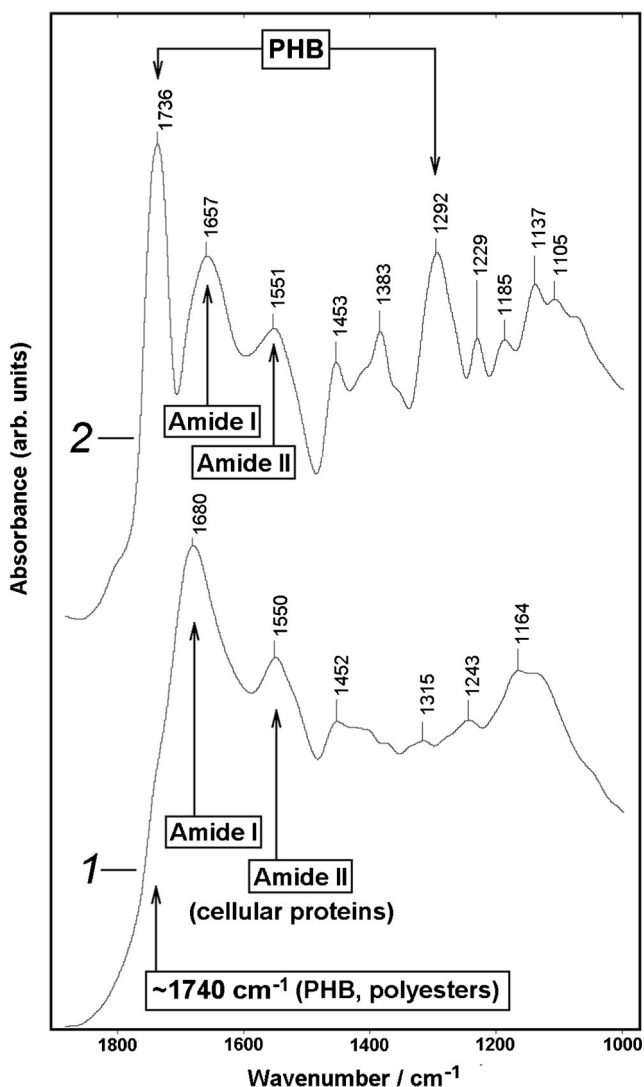


**Fig. 1** Diffuse reflectance infrared Fourier transform (DRIFT) spectra of *Azospirillum brasilense* strain Sp7 cells (1) grown for 18 h with  $0.5 \text{ g l}^{-1}$   $\text{NH}_4\text{Cl}$  and lyophilised, as well as of dried cell biomass used for comparison [11] (2) similarly grown under nutritional stress (2 d; without  $\text{NH}_4\text{Cl}$ ). The positions of main bands of cellular proteins, amide I and amide II, and of the most pronounced bands related to poly-3-hydroxybutyrate (PHB, intracellular storage polyester) [11, 22] are indicated with arrows

microaerophilic [6], nevertheless, grow relatively well also under aeration [22]. The DRIFT spectrum of the dried biomass obtained in this study as described in the previous section (Fig. 1, spectrum 1) was found to closely match the DRIFT spectrum of the *A. brasilense* Sp7 grown without nutritional stress [11] and to significantly differ from the spectrum of the biomass grown under bound-nitrogen limitation (without  $\text{NH}_4\text{Cl}$ ; see Fig. 1, spectrum 2). In particular, in the vibration region featuring the main intensive absorption bands of cellular proteins (within ca.  $1700\text{--}1500 \text{ cm}^{-1}$ ) [7, 10, 22, 26], the amide I and amide II bands in the sample under study (see Fig. 1, spectrum 1) dominate, while the biomass grown under

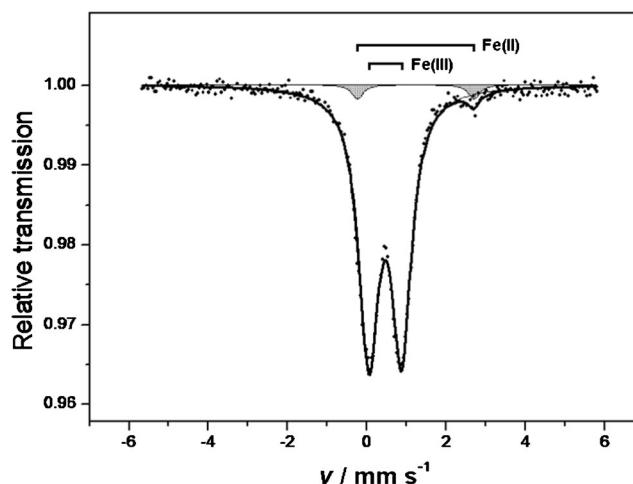


**Fig. 2** Mössbauer spectrum (measured at  $T=80 \text{ K}$ ) of *A. brasilense* Sp7 dry biomass (grown for 18 h with  $^{57}\text{Fe}^{\text{III}}\text{-NTA}$  complex as a sole source of iron, separated by centrifugation, immediately frozen in liquid nitrogen and lyophilised; see also Table 1). The positions of the quadrupole doublets corresponding to  $\text{Fe}^{\text{II}}$  and  $\text{Fe}^{\text{III}}$  components are shown by square brackets above the spectrum. These spectral components (quadrupole doublets) represent the contributions of  $\text{Fe}^{\text{III}}$  (non-shaded area) or  $\text{Fe}^{\text{II}}$  (shaded area) to the whole spectrum area (defined by the outer solid-line envelope) calculated by fitting the experimental data (points)

nutritional stress shows a completely different DRIFT spectrum with prominent bands of intracellularly accumulated poly-3-hydroxybutyrate (PHB; see spectrum 2) [11]. Therefore, under the cultivation conditions applied for the sample under study, *A. brasilense* Sp7 cells were not subjected to any appreciable nutritional stress (e.g. bound-nitrogen deficiency) which could induce PHB accumulation [7, 10, 11, 22]. Thus, the biomass prepared for Mössbauer measurements was evidently in its common (unstressed) state.

A Mössbauer spectrum (measured at  $T=80 \text{ K}$ ) obtained for the dry biomass of *A. brasilense* Sp7 (frozen immediately after 18 h of growth in the culture medium and lyophilised) is shown in Fig. 2 (the calculated Mössbauer parameters are listed in Table 1). It consists of a dominating quadrupole doublet of a high-spin ferric component with somewhat broadened lines and a small contribution of a high-spin ferrous component. The ferric component ( $\delta=0.46 \text{ mm s}^{-1}$ ;  $\Delta=0.82 \text{ mm s}^{-1}$ ) with a slightly increased linewidth (over  $0.5 \text{ mm s}^{-1}$ ) could be attributed to bacterial ferritin-like components similar to those observed for other microorganisms [27–29]; the increased linewidth corresponds to the heterogeneity of the hydrous iron oxyhydroxide ferritin core [19]. As for a variety of ferritin species in bacteria, comprehensive descriptions of their structures, functions and bionanotechnological applications have recently been reviewed [20, 21].

The minor ferrous component (3–4 %, see Table 1) can be associated with  $\text{Fe}^{\text{II}}$  originated from the intracellular reduction of iron(III) from the  $\text{Fe}^{\text{III}}\text{-NTA}$  complex contained in the culture medium [17, 18]. On the other hand, note that in whole-

**Table 1** Mössbauer parameters calculated from the spectra (see Figs. 2 and 3) for *A. brasilense* Sp7 dry biomass (grown for 18 h with  $^{57}\text{Fe}^{\text{III}}$ -NTA complex as a sole source of iron, separated by centrifugation, immediately frozen in liquid nitrogen and lyophilised)

Parameter <sup>a</sup>	$T=80\text{ K}$	$T=5\text{ K}$ No external field	$T=2\text{ K}$ No external field	$T=2\text{ K}$ $B_{\text{ext}}=5\text{ T}$
Magnetic component				
$A$	–	73 ( <i>I</i> ) <sup>b</sup>	80 ( <i>I</i> ) <sup>c</sup>	83 ( <i>I</i> ) <sup>d</sup>
$\delta$		0.48 (1)	0.50 (1)	0.48 (1)
$B$		48.2 (5)	47.9 (5)	47.0 (5)
Doublet $\text{Fe}^{3+}$				
$A$	97 ( <i>I</i> )	23 ( <i>I</i> )	18 ( <i>I</i> )	17 ( <i>I</i> )
$\delta$	0.46 (2)	0.44 (1)	0.44 (1)	0.43 <sup>e</sup>
$\Delta$	0.82 (3)	0.94 (2)	0.90 (2)	1.16 (6)
$W$	0.59 (5)	0.77 (4)	0.70 (3)	1.26 (1)
Doublet $\text{Fe}^{2+}$				
$A$	3 ( <i>I</i> )	4 ( <i>I</i> )	2 ( <i>I</i> )	1 ( <i>I</i> )
$\delta$	1.23 (2)	1.39 (4)	1.41 (6)	1.38 (6)
$\Delta$	2.94 (4)	3.24 (7)	3.3 (1)	3.7 (3)
$W$	0.34 <sup>e</sup>	0.6 <sup>e</sup>	0.6 <sup>e</sup>	0.6 <sup>e</sup>

All the  $A$  values (italicised) are significant (they represent the relative areas of the corresponding components, in % of the total spectrum area; their sum in each column for all the components gives ~100%)

<sup>a</sup>  $\delta$ , isomer shift ( $\text{mm s}^{-1}$  relative to  $\alpha\text{-Fe}$  at room temperature);  $\Delta$ , quadrupole splitting ( $\text{mm s}^{-1}$ );  $W$ , linewidth ( $\text{mm s}^{-1}$ ; full width at half maximum);  $B$ , internal or effective magnetic field (T);  $A$ , relative area of a spectral component (%); calculated errors (in the last digit) are given in brackets

<sup>b</sup> Linewidths:  $1.53\text{ mm s}^{-1}$ ,  $1.42\text{ mm s}^{-1}$ ,  $0.9\text{ mm s}^{-1}$

<sup>c</sup> Linewidths:  $1.48\text{ mm s}^{-1}$ ,  $1.29\text{ mm s}^{-1}$ ,  $0.9\text{ mm s}^{-1}$

<sup>d</sup> Linewidths:  $1.73\text{ mm s}^{-1}$ ,  $1.53\text{ mm s}^{-1}$ ,  $0.5\text{ mm s}^{-1}$

<sup>e</sup> Fixed values during the fitting

cell Mössbauer studies of microorganisms, the  $\text{Fe}^{\text{II}}$  levels were reported to be from a few percent up to half of total cellular iron, depending on various factors, particularly on the levels of total cellular iron [30]. In particular, it has been shown that many aspects of  $\text{Fe}^{\text{II}}$ -to- $\text{Fe}^{\text{III}}$  oxidation at ferroxidase centres in bacterial ferritins and the mechanisms of  $\text{Fe}^{\text{III}}$  displacement from the binding sites, transfer to the ferritin cavity and the formation of the ferric core are still not completely understood, as several models are still under discussion [20]. We also would like to note that, despite the availability of numerous structural studies of various ferritins by Mössbauer spectroscopy and other modern instrumental techniques (see, e.g. [19–21, 31–37] and references therein), different models for the ferritin core structure have so far been suggested ranging from monocrystalline to polycrystalline and to polyphasic with different degrees of crystallinity [37]. On the basis of the data available so far, it may be reasoned that the structure of ferritin cores is consistent with heterogeneous and multiphase models, rather than with a simple core-shell model.

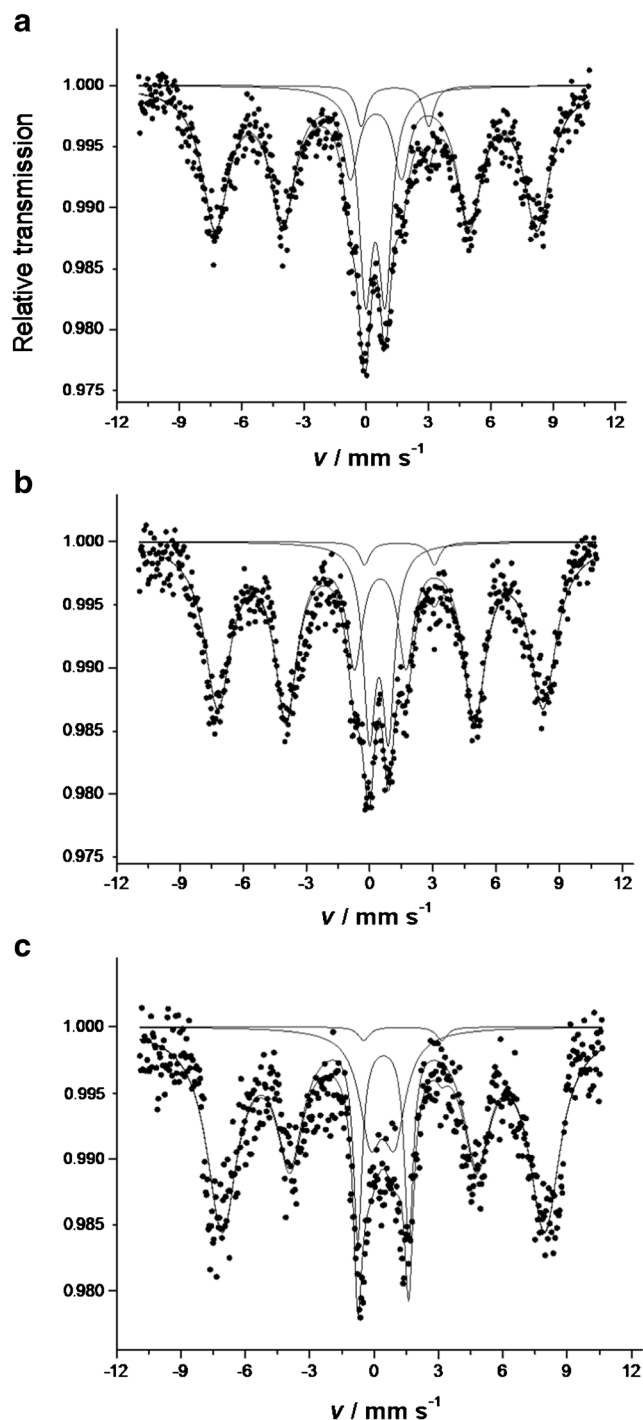


**Fig. 3** Mössbauer spectra of *A. brasilense* Sp7 dry biomass (grown for 18 h with  $^{57}\text{Fe}^{\text{III}}$ -NTA complex as a sole source of iron, separated by centrifugation, immediately frozen in liquid nitrogen and lyophilised; see also Table 1) measured at **a**  $T=5\text{ K}$  and **b**  $T=2\text{ K}$  (without an external field), as well as **c** at  $T=2\text{ K}$  in an external field  $B_{\text{ext}}=5\text{ T}$ . The spectral components (quadrupole doublets and magnetically split sextets, shown by *thin solid lines*) represent the contributions of different forms of  $\text{Fe}^{\text{III}}$  or  $\text{Fe}^{\text{II}}$  (see Table 1) to the whole spectrum area (defined by the *outer solid-line envelope*) calculated by fitting the experimental data (points)

In order to elucidate the correct assignment of the dominant ferric component found at 80 K (see Fig. 2), low-temperature

and in-field Mössbauer spectroscopy was applied (Fig. 3; see also Table 1). At a low temperature (<10 K), the Mössbauer spectrum of ferritin exhibits a typical magnetically split pattern with characteristic Mössbauer parameters due to the antiferromagnetic [38] (and a possible sperimagnetic [39]) coupling between the iron atoms in the ferrihydrite core of ferritin. In-field Mössbauer spectroscopy can reveal the nature of the magnetic coupling, i.e. whether the material is ferromagnetic, ferrimagnetic or antiferromagnetic. By applying an external magnetic field, the antiferromagnetic coupling can be well identified, since, in the case of a polycrystalline antiferromagnet, the application of an external magnetic field would usually have no effect on the hyperfine field.

A dominant magnetically split component ( $A=73\%$ , see Table 1) appeared in the spectrum recorded at 5 K (Fig. 3a). This sextet originated from the partial transformation of the broadened quadrupole doublet (97 % of total cellular Fe) observed at 80 K (see Fig. 2 and Table 1). The sextet shows a bacterial ferritin species accumulated in the bacterial cells, since the Mössbauer parameters of the magnetically split component correspond to those obtained earlier for the bacterial ferritin [40].

In the spectrum recorded at  $T=2$  K without an external magnetic field (Fig. 3b), the relative occurrence of the magnetic component increases ( $\sim 80\%$ ), which shows the superparamagnetic nature of ferritin species due to small particle sizes of the ferric core. A wide distribution of particle sizes can be estimated from the comparison of spectra recorded at different temperatures. The magnetic ordering at low temperatures is well known for bacterial ferritins since the ferrihydrite incorporated in the protein structure is poorly ordered, nano-sized, and hence its superparamagnetic blocking temperature is low [40, 41].

The Mössbauer spectrum of the bacterial cells at 2 K in a 5 T external magnetic field (Fig. 3c) exhibited a similar sextet as found at 2 K without an applied magnetic field (see Fig. 3b) with the same effective magnetic field within the experimental error (see Table 1). (Note that the corresponding Mössbauer parameters at 5 and 2 K are almost the same within the instrumental error [42].) This demonstrates the existence of an antiferromagnetic coupling between the iron atoms (when the external magnetic field does not change the effective magnetic field). Consequently, the assignment of the sextet component to ferritin is evidently proven by the spectrum recorded at 2 K when an external magnetic field of 5 T was applied, since the Mössbauer parameters of the sextet are consistent with the expectation for an external magnetic field applied to antiferromagnetic ferritin particles.

The minor paramagnetic component (decreasing from 23 to 17–18 % of total cellular iron in going from  $T=5$  K to  $T=2$  K) may belong to ferric complexes other than the ferritin core [20, 30], although it cannot be excluded that this part also belongs to superparamagnetic ferritin species with core sizes smaller than in those superparamagnetic at  $\geq 2$  K.

The change in the relative intensity of the second and fifth lines of the magnetically split sextet induced by the applied external magnetic field can be associated with some small sperimagnetism [39] and/or a small change in the magnetic character of ferrihydrite nanoparticles coated [43] by the protein shell in ferritin macromolecules, which does not influence the Mössbauer spectroscopic assignment. (Note that the relatively low signal-to-noise ratio related to a low cellular  $^{57}\text{Fe}$  content did not allow a further decomposition of the magnetically split component which could give more detailed information on the iron core of ferritin.)

The  $\text{Fe}^{\text{II}}$  component with the very small relative concentration, detected in the 80 K spectrum ( $\sim 3 \pm 1\%$ ), can also be observed in these low-temperature spectra (see Fig. 3 and Table 1). This residual high-spin ferrous iron evidently represents the  $\text{Fe}^{\text{II}}$  originated from the intracellular iron(III) reduction, while the presence of non-oxidised  $\text{Fe}^{\text{II}}$  bound within ferroxidase iron-binding centres in bacterial ferritin [20] cannot be excluded.

## Conclusions

Low-temperature Mössbauer spectroscopic data with and without an applied external magnetic field have evidenced the occurrence of ferritin as dominant iron-bearing species in the rhizobacterium *A. brasilense* Sp7. The remaining iron species are represented by a high-spin iron(III) component superparamagnetic down to  $T=2$  K (ca. 20 % of total cellular iron) and a few percent of high-spin iron(II) complexes.

**Acknowledgements** This study was supported in parts by Project LO1305 of the Ministry of Education, Youth and Sports of the Czech Republic and by The Russian Foundation for Basic Research (Grant No. 13-04-01538-a), as well as under the Agreement on Scientific Cooperation between the Russian and Hungarian Academies of Sciences for 2011–2013 (Projects Nos. 28 and 29).

## Compliance with ethical standards

**Conflict of interest** The authors declare that the research was conducted in the absence of any commercial or financial relationships that could be construed as a potential conflict of interest.

## References

1. Bashan Y, de-Bashan LE, Prabhu SR, Hernandez J-P. Advances in plant growth-promoting bacterial inoculant technology: formulations and practical perspectives (1998–2013). *Plant Soil*. 2014;378:1–33.
2. Wisniewski-Dyé F, Drogue B, Borland S, Prigent-Combaret C. *Azospirillum*-plant interaction: from root colonisation to plant growth promotion. In: Belén Rodelas González M, González-López J, editors. *Beneficial plant-microbial interactions: ecology*

- and applications, vol. Chapter 11. Boca Raton: CRC Press; 2013. p. 237–69.
3. Bashan Y, de-Bashan LE. How the plant growth-promoting bacterium *Azospirillum* promotes plant growth—a critical assessment. *Adv Agron*. 2010;108:77–136.
  4. Veresoglou SD, Menexes G. Impact of inoculation with *Azospirillum* spp. on growth properties and seed yield of wheat: a meta-analysis of studies in the ISI Web of science from 1981 to 2008. *Plant Soil*. 2010;337:469–80.
  5. Rothballer M, Schmid M, Hartmann A. In situ localization and PGPR-effect of *Azospirillum brasilense* strains colonizing roots of different wheat varieties. *Symbiosis*. 2003;34:261–79.
  6. Bashan Y, Holguin G, de-Bashan LE. *Azospirillum*-plant relationships: physiological, molecular, agricultural, and environmental advances (1997–2003). *Can J Microbiol*. 2004;50:521–77.
  7. Kamnev AA, Tugarova AV, Antonyuk LP, Tarantilis PA, Kulikov LA, Perfiliev YuD, et al. Instrumental analysis of bacterial cells using vibrational and emission Mössbauer spectroscopic techniques. *Anal Chim Acta*. 2006;573–574:445–52.
  8. Mulyukin AL, Suzina NE, Pogorelova AY, Antonyuk LP, Duda VI, El'-Registan GI. Diverse morphological types of dormant cells and conditions for their formation in *Azospirillum brasilense*. *Microbiology*. 2009;78:33–41.
  9. Pogorelova AY, Mulyukin AL, Antonyuk LP, Galchenko VF, El'-Registan GI. Phenotypic variability in *Azospirillum brasilense* strains Sp7 and Sp245: association with dormancy and characteristics of the variants. *Microbiology*. 2009;78:559–68.
  10. Kamnev AA, Tugarova AV, Tarantilis PA, Gardiner PHE, Polissiou MG. Comparing poly-3-hydroxybutyrate accumulation in *Azospirillum brasilense* strains Sp7 and Sp245: the effects of copper(II). *Appl Soil Ecol*. 2012;61:213–6.
  11. Kamnev AA, Tugarova AV, Kovács K, Kuzmann E, Biró B, Tarantilis PA, et al. Emission ( $^{57}\text{Co}$ ) Mössbauer spectroscopy as a tool for probing speciation and metabolic transformations of cobalt(II) in bacterial cells. *Anal Bioanal Chem*. 2013;405:1921–7.
  12. Cassán FD, Okon Y, Creus CM, editors. *Handbook for Azospirillum*. Technical issues and protocols. Basel: Springer; 2015. doi:10.1007/978-3-319-06542-7.
  13. Barton LL, Johnson GV, Bishop YM. The metabolism of iron by nitrogen-fixing rhizospheric bacteria. In: Barton LL, Abadia J, editors. *Iron nutrition in plants and rhizospheric microorganisms*, vol. Chapter 9. Dordrecht: Springer; 2006. p. 199–214.
  14. Bachhawat AK, Ghosh S. Iron transport in *Azospirillum brasilense*: role of the siderophore spirilobactin. *J Gen Microbiol*. 1987;133:1759–65.
  15. Mori E, Fulchieri M, Indorato C, Fani R, Bazzicalupo M. Cloning, nucleotide sequencing, and expression of the *Azospirillum brasilense lon* gene: involvement in iron uptake. *J Bacteriol*. 1996;178(12):3440–6.
  16. Kamnev AA, Renou-Gonnord M-F, Antonyuk LP, Colina M, Chernyshev AV, Frolov I, et al. Spectroscopic characterization of the uptake of essential and xenobiotic metal cations in cells of the soil bacterium *Azospirillum brasilense*. *IUBMB Life*. 1997;41:123–30. doi:10.1080/15216549700201121.
  17. Kamnev AA, Tugarova AV, Kovács K, Kuzmann E, Homonnay Z, Kulikov LA, et al. Mössbauer spectroscopic study of iron and cobalt metabolic transformations in cells of the bacterium *Azospirillum brasilense* Sp7. *Bull Russ Acad Sci Phys*. 2015;79(8):1036–40. doi:10.3103/S1062873815080110.
  18. Kamnev AA, Tugarova AV, Kovács K, Biró B, Homonnay Z, Kuzmann E. Mössbauer spectroscopic study of  $^{57}\text{Fe}$  metabolic transformations in the rhizobacterium *Azospirillum brasilense* Sp245. *Hyperfine Interact*. 2014;226:415–9.
  19. Alenkina IV, Oshtrakh MI, Tugarova AV, Biró B, Semionkin VA, Kamnev AA. Study of the rhizobacterium *Azospirillum brasilense* Sp245 using Mössbauer spectroscopy with a high velocity resolution: Implication for the analysis of ferritin-like iron cores. *J Mol Struct*. 2014;1073:181–6.
  20. Honarmand Ebrahimi K, Hagedoorn P-L, Hagen WR. Unity in the biochemistry of the iron-storage proteins ferritin and bacterioferritin. *Chem Rev*. 2015;115:295–326.
  21. Jutz G, van Rijn P, Miranda BS, Böker A. Ferritin: a versatile building block for bionanotechnology. *Chem Rev*. 2015;115:1653–701.
  22. Kamnev AA, Sadovnikova JN, Tarantilis PA, Polissiou MG, Antonyuk LP. Responses of *Azospirillum brasilense* to nitrogen deficiency and to wheat lectin: a diffuse reflectance infrared Fourier transform (DRIFT) spectroscopic study. *Microb Ecol*. 2008;56:615–24.
  23. Pechoušek J, Jančík D, Frydrych J, Navařík J, Novák P. Setup of Mössbauer spectrometers at RCPTM. *AIP Conf Proc*. 2012;1489:186–93. doi:10.1063/1.4759489.
  24. Pechoušek J, Prochazka R, Jančík D, Frydrych J, Mashlan M. Universal LabVIEW-powered Mössbauer spectrometer based on USB PCI or PXI devices. *J Phys Conf Ser*. 2010;217:012006. doi:10.1088/1742-6596/217/1/012006.
  25. Klencsár Z, Kuzmann E, Vértes A. User-friendly software for Mössbauer spectrum analysis. *J Radioanal Nucl Chem*. 1996;210:105–18.
  26. Naumann D. Infrared spectroscopy in microbiology. In: Meyers RA, editor. *Encyclopedia of analytical chemistry*. Chichester: Wiley; 2000. p. 102–31.
  27. Hartnett A, Böttger LH, Matzanke BF, Carrano CJ. A multidisciplinary study of iron transport and storage in the marine green alga *Tetraselmis suecica*. *J Inorg Biochem*. 2012;116:188–94.
  28. Winkler H, Meyer W, Trautwein AX, Matzanke BF. Mössbauer and EXAFS studies of bacterioferritin from *Streptomyces olivaceus*. *Hyperfine Interact*. 1994;91:841–6.
  29. Matzanke BF, Bill E, Müller GI, Winkelmann G, Trautwein AX. In vivo Mössbauer spectroscopy of iron uptake and ferrometabolism in *Escherichia coli*. *Hyperfine Interact*. 1989;47:311–27.
  30. Andrews SC. Iron storage in bacteria. *Adv Microb Physiol*. 1998;40:281–351.
  31. Gálvez N, Fernández B, Sánchez P, Cuesta R, Ceolín M, Clemente-León M, et al. Comparative structural and chemical studies of ferritin cores with gradual removal of their iron contents. *J Am Chem Soc*. 2008;130(25):8062–8.
  32. Pan Y-H, Sader K, Powell JJ, Bleloch A, Gass M, Trinick J, et al. 3D morphology of the human hepatic ferritin mineral core: new evidence for a subunit structure revealed by single particle analysis of HAADF-STEM images. *J Struct Biol*. 2009;166(1):22–31.
  33. Papaefthymiou GC. The Mössbauer and magnetic properties of ferritin cores. *Biochim Biophys Acta*. 1800;2010:886–97.
  34. Lopez-Castro JD, Delgado JJ, Perez-Omil JA, Gálvez N, Cuesta R, Watt RK, et al. A new approach to the ferritin iron core growth: influence of the H/L ratio on the core shape. *Dalton Trans*. 2012;41(4):1320–4.
  35. Alenkina IV, Oshtrakh MI, Klepova YuV, Dubiel SM, Sadovnikov NV, Semionkin VA. Comparative study of the iron cores in human liver ferritin, its pharmaceutical models and ferritin in chicken liver and spleen tissues using Mössbauer spectroscopy with a high velocity resolution. *Spectrochim Acta Part A: Mol Biomol Spectrosc*. 2013;100:88–93.
  36. Kamnev AA, Kovács K, Alenkina IV, Oshtrakh MI. Mössbauer spectroscopy in biological and biomedical research. In: Sharma VK, Klingelhöfer G, Nishida T, editors. *Mössbauer spectroscopy: applications in chemistry, biology, and nanotechnology*, vol. Chapter 13. N.Y.: Wiley; 2013. p. 272–91.
  37. Alenkina IV, Oshtrakh MI, Klencsár Z, Kuzmann E, Chukin AV, Semionkin VA.  $^{57}\text{Fe}$  Mössbauer spectroscopy and electron paramagnetic resonance studies of human liver ferritin, *Ferrum Lek*

- and Maltofer®. *Spectrochim Acta Part A: Mol Biomol Spectrosc.* 2014;130:24–36.
38. Pankhurst QA, Pollard RJ. Structural and magnetic properties of ferrihydrite. *Clays Clay Miner.* 1992;40(3):268–72. doi:10.1346/CCMN.1992.0400303.
  39. Coey JMD, Readman PW. Characterisation and magnetic properties of natural ferric gel. *Earth Planet Sci Lett.* 1973;21(1):45–51. doi:10.1016/0012-821X(73)90224-0.
  40. St Pierre TG, Bell SH, Dickson DPE, Mann S, Webb J, Moore GR, et al. Mössbauer spectroscopic studies of the cores of human, limpet and bacterial ferritins. *Biochim Biophys Acta Protein Struct Mol Enzymol.* 1986;870(1):127–34.
  41. Cornell RM, Schwertmann U. *The iron oxides: structure, properties, reactions, occurrences and uses.* 2nd ed. Weinheim: Wiley-VCH; 2003.
  42. Oshtrakh MI, Semionkin VA. Mössbauer spectroscopy with a high velocity resolution: advances in biomedical, pharmaceutical, cosmochemical and nanotechnological research. *Spectrochim Acta Part A: Mol Biomol Spectrosc.* 2013;100:78–87.
  43. Berquó TS, Erbs JJ, Lindquist A, Penn RL, Banerjee SK. Effects of magnetic interactions in antiferromagnetic ferrihydrite particles. *J Phys Condens Matter.* 2009;21(17):176005. doi:10.1088/0953-8984/21/17/176005.